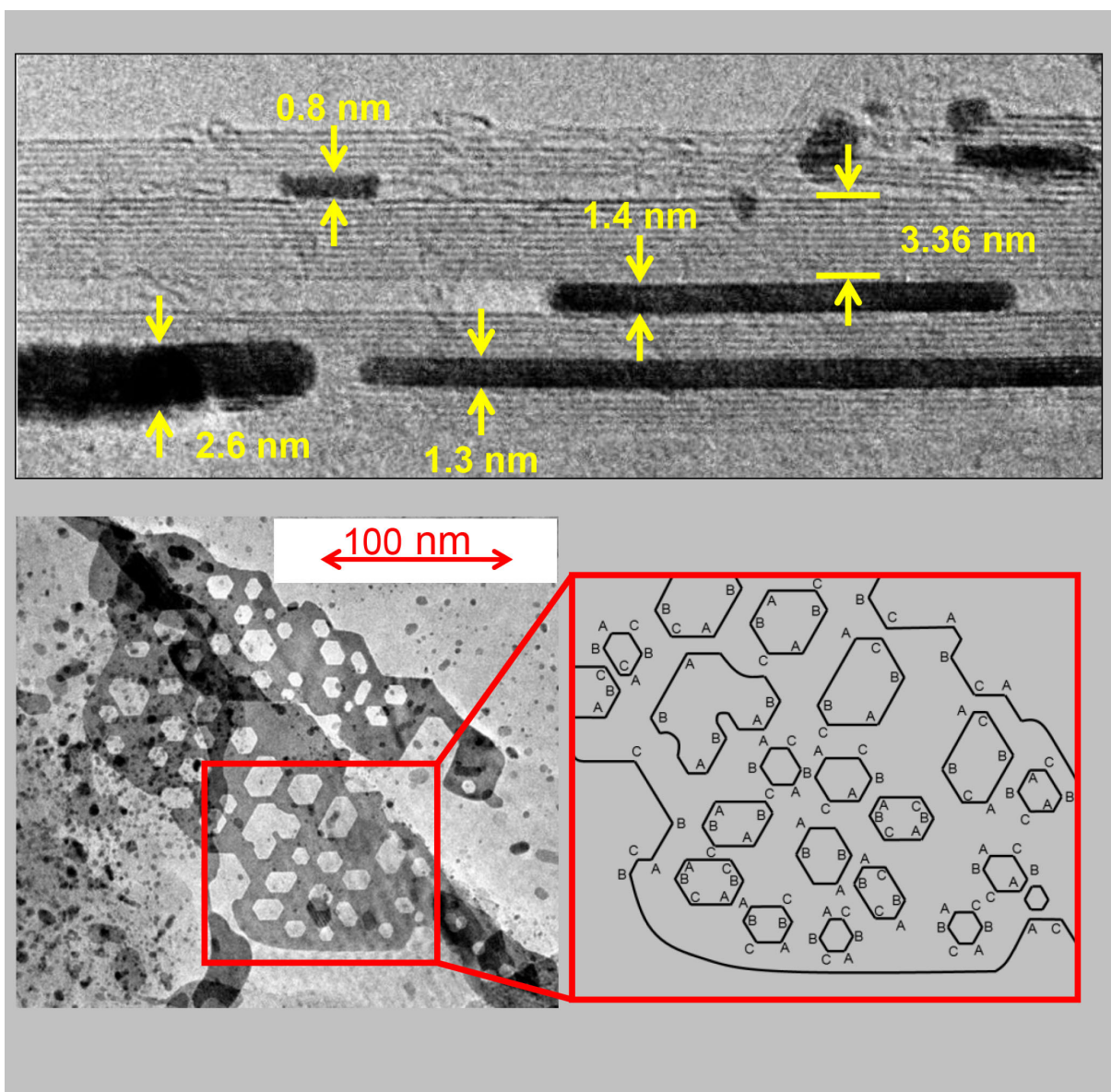


Platinum Nanosheets between Graphite Layers

Masayuki Shirai*^[a]



Abstract: Two-dimensional platinum nanosheets were obtained by the hydrogen reduction of platinum tetrachloride intercalated between graphite layers, the latter was prepared by the treatment of the mixture of platinum tetrachloride and graphite powder under chlorine atmosphere. The size of platinum nanosheets was 1–3 nm in thickness with a width in the range of 5–300 nm. These nanosheets contain a number of hexagonal holes and edges with an angle of 120°. This review discusses the reduction and oxidation behavior of platinum species and structure of platinum nanosheets between graphite layers. The selective hydrogenation catalyzed by these platinum nanosheets entrapped between the graphite layers is also demonstrated.

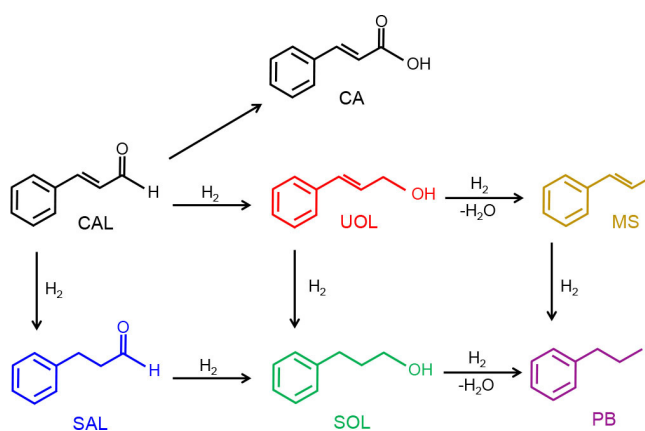
Keywords: Nanoparticles, Intercalations, Layered compounds, Hydrogenation

1. Introduction

Graphite has a layered structure consisting of a regular hexagonal network of carbon atoms which are conjugated with sp^2 hybrid orbitals. A variety of chemical substances can be inserted into the interlayer spaces of graphite to produce graphite intercalated compounds (GICs), because graphite layers can accept or donate electrons from the substrates and the interaction between graphite layers is of weak van der Waals force.^[1] Metal chloride can be intercalated between graphite layers (MClx-GIC) by the treatment of metal chloride and graphite powder under vacuum or high-pressure chlorine.^[1]

The reduction of MClx-GIC is expected to produce nanometal particles intercalated between two-dimensional graphite layers. Several reports are available on the formation of metal particles located in graphite layers e.g. Klotz and Schneider reported that Fe metal between graphite layers could be prepared by the reduction of iron chloride (III) intercalated between graphite layers by sodium in liquid ammonia.^[2] Vol'pin et al. also reported that entrapping transition metal particles (Co, Ni, Mn, Cu, Mo, and Cr) between graphite layers could be achieved by the reduction of the corresponding metal chloride intercalated between graphite layers.^[3] Graphite-intercalated metal particles (Fe, Co, Cu, Ni, and Pd) commercially available in 1980's (Graphimet) were prepared by the treatment of MClx-GIC with lithium biphenyl at 223 K under helium atmosphere. Graphimets were used as solid catalysts; however, their activities were not so high compared with the conventional catalysts, because active metal sites were encapsulated between graphite layers to which substrate should have an easy access for adsorption.^[4–9] Walter et al. reported that small and plate-like Pd metal particles inserted into the graphite layers could be obtained by the reduction of palladium chloride (II) intercalated graphite powder in hydrogen atmosphere.^[10,11]

The above reports show that the formation of metal particles between graphite layers had small or plate-like structure with 1–10 nm sizes. There are few reports on the formation of large two-dimensional metal sheets with nanometer size thickness between graphite layers.



Scheme 1. Hydrogenation of cinnamaldehyde (CAL).

The preparation, structure and catalysis of two-dimensional platinum nanosheets between graphite layers are reported in this review. The platinum nanosheets were prepared by the hydrogen reduction of platinum chloride intercalated between graphite layers (PtClx-GIC). The size of platinum nanosheets were 1–3 nm in thickness with 5–300 nm width. There are a number of hexagonal holes and edges with 120° angle, which were formed during reduction of platinum chloride intercalated between graphite layers by hydrogen atmosphere. The platinum nanosheets intercalated between graphite layers (Pt-GIC) showed selective hydrogenation activity, especially, the selectivities over platinum nanosheets sandwiched between graphite layers were different from those over platinum metal particles supported on graphite layers.

[a] Prof. M. Shirai

Faculty of Science and Engineering
Iwate University
4-3-5 Ueda, Morioka, Iwate 020-8551
E-mail: mshirai@iwate-u.ac.jp

2. Experimental

2.1. Preparation of Platinum Nanosheets

The treatment with chlorine gas under high pressure and high temperature conditions is needed for the insertion of metal chloride into graphite layers. Figure 1 shows the apparatus for the preparation of GICs, which is made of SUS tubes and a quartz reactor.

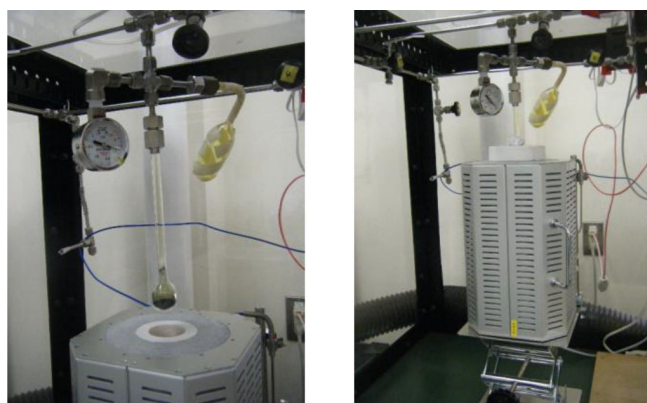


Figure 1. Apparatus for preparation of GICs with high pressure chlorine.

The connection between a SUS tube and a quartz reactor was sealed with a Teflon packing. The mixture of graphite powder and platinum chloride (Aldrich, 99.99%) was mixed under high pressure of 0.3 MPa of chlorine to prepare platinum chloride intercalated graphite compound (PtCl_x-GIC).^[12,13] The platinum loading in weight percent is indicated by a value prefixed before the sample name, viz. 5PtCl_x-GIC shows 5 wt% of platinum metal is loaded in the sample.

The platinum chloride between graphite layers was reduced by 40 kPa of hydrogen at 423–773 K in a batch system to produce platinum metal intercalated between graphite layers (Pt-GIC).

2.2. Hydrogenation Catalysis of Platinum Nanosheets

The catalytic performance of Pt-GIC in organic solvents was studied in a batch system using stainless-steel reactor (50 ml capacity). For the hydrogenation in supercritical carbon dioxide solvent also, a batch system of stainless-steel reactor was adopted.^[14,15] The weighed amounts of catalyst and the reactant were placed in a reactor and flushed twice with carbon dioxide. After the required temperature was attained with a hot air circulating oven, hydrogen and carbon dioxide were introduced into the reactor. The carbon dioxide pressure values were determined by the subtraction of hydrogen pressure from the total pressure. After the appropriate reaction time, the pressure was released slowly and the contents were discharged to separate the catalyst by simple filtration. The products dissolved in acetone were analyzed by a gas chromatograph.

2. Platinum Nanosheets Between Graphite Layers

2.1. Intercalation of Platinum Chloride

Figure 2 shows X-ray diffraction patterns of graphite (KS6 purchased from TIMCAL TIMREX) and the prepared sample. New peaks at $2\theta = 10.0^\circ$, 14.6° , and 20.3° were observed for 5PtCl_x-GIC (Figure 2(b)) in addition to the characteristic peaks of graphite structure (Figure 2(a)).

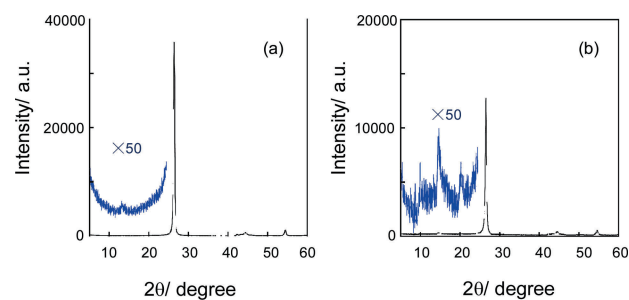


Figure 2. XRD patterns of graphite(a) and 5PtCl_x-GIC(b).

These new three peaks are in good agreement with the diffraction peak positions calculated for (002), (003), and



Masayuki SHIRAI received Ph.D. at University of Tokyo in 1993. After working as an associate professor at Tohoku University and as a team leader at National Institute of Advanced Industrial Science and Technology (AIST), he has been a full professor of Iwate University since 2013. His research interest is green chemistry using supported metal catalysts in carbon dioxide and/or water solvents under high-pressure including supercritical conditions.

(004) reflections from the repeat distance along the *c* axis ($c = 1.76$ nm), which are at $2\theta = 10.0^\circ$, 15.1° , and 20.2° , respectively, indicating that the 5PtClx-GIC sample has a stage three structure, in which one intercalant layer of 0.75 nm exists between every three graphite layers (0.336 nm). Platinum tetrachloride, which has a layered structure,^[16] would be intercalated in the graphite layer. A proposed structure of PtClx-GIC is shown in Figure 3. Figure 4 shows a TEM image of 5PtClx-GIC, in which small platinum metal particles are formed. The PtClx-GIC samples are not stable in methanol as platinum chloride from graphite dissolved in methanol. The image was obtained with a TEM mesh which was prepared by direct sprinkling of platinum chloride powder. The TEM image shows that small platinum metal particles, which would be formed by the reduction of platinum chloride under the irradiation of electron beam during TEM observation.^[17] Figure 4 shows that platinum chloride species were inhomogeneously dispersed. Platinum chloride species would not be homogeneously intercalated and be eccentrically located between the two-dimensional graphite layers, then the platinum metal particles formed by the irradiation would be located in the graphite layers.

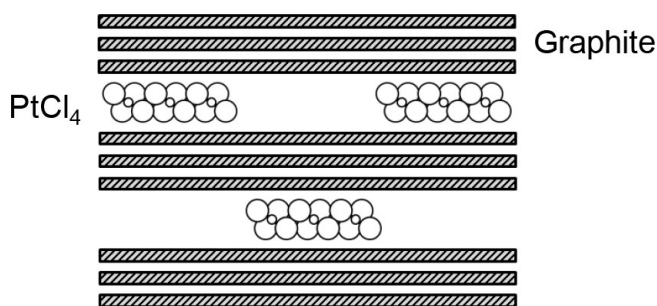


Figure 3. A proposed structure of PtClx-GIC.

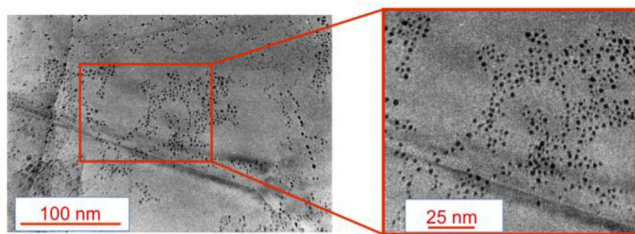


Figure 4. A TEM image of 5PtClx-GIC.

Figure 5 shows the intensities of a peak at $2\theta = 26.6^\circ$ (graphite (002)) and a peak at $2\theta = 10.0^\circ$ of the PtClx-GIC samples as a function of platinum loadings. With an increase in amount of platinum tetrachloride inserted, three peaks become stronger, while the diffraction for (002) of graphite

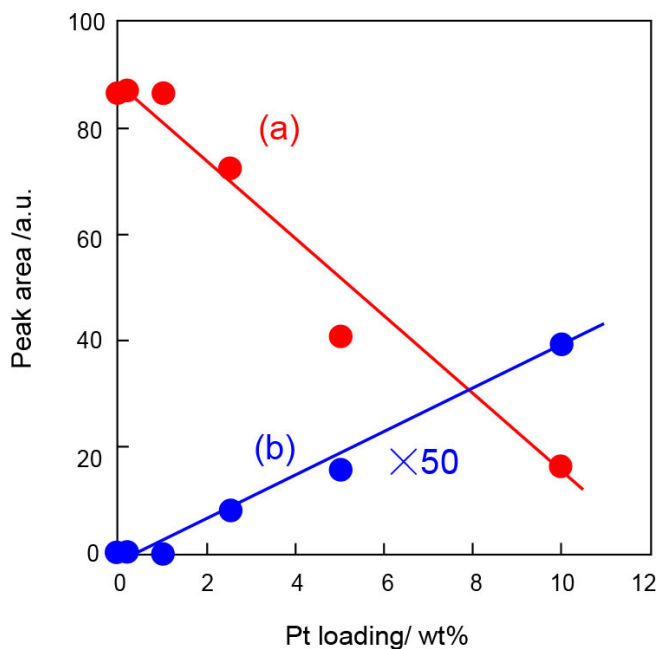


Figure 5. The XRD peak intensities of graphite at 26.6° (a) and PtClx-GIC at 10.0° (b).

becomes weaker. No other peaks except for the three peaks and graphite peaks were observed indicating that the PtClx-GIC samples have two domains; one is “pure” graphite matrix and the other platinum chloride intercalated graphite with the stage three structure. The latter should increase with an increase in the amount of platinum chloride inserted.

2.2. Platinum Nanosheets

Figure 6 shows TEM images of the 5Pt-GIC sample obtained by JEOL JEM-2100 (200 keV). XMA analysis confirmed that the dark images were composed of platinum. Figures 6(a)-(c) are TEM images of 5Pt-GIC. Several rod-like platinum images in parallel are seen in Figure 6(a) while, sheet-like platinum images with hexagonal holes are seen in Figure 6(c). The TEM analysis with the rotation of the Pt-GIC sample against electron beam confirmed that the rod-like images shown in Figure 6(a) was a side view and (c) was a top view of the platinum nanosheets intercalated between graphite layers. The platinum sheets are arranged in parallel with graphite layers (interlayer distance of 0.335 nm) in Figure 6(b), which is the magnified view of Figure 6(a). Void spaces are also observed at the edge of the platinum sheets. Figure 6(d) is a drawing of the top view of platinum sheet. The AB side of the hexagonal holes in the platinum sheet are straight and parallel to each other. The BC and AC sides in the hexagonal holes and edges at the sheet are also parallel to

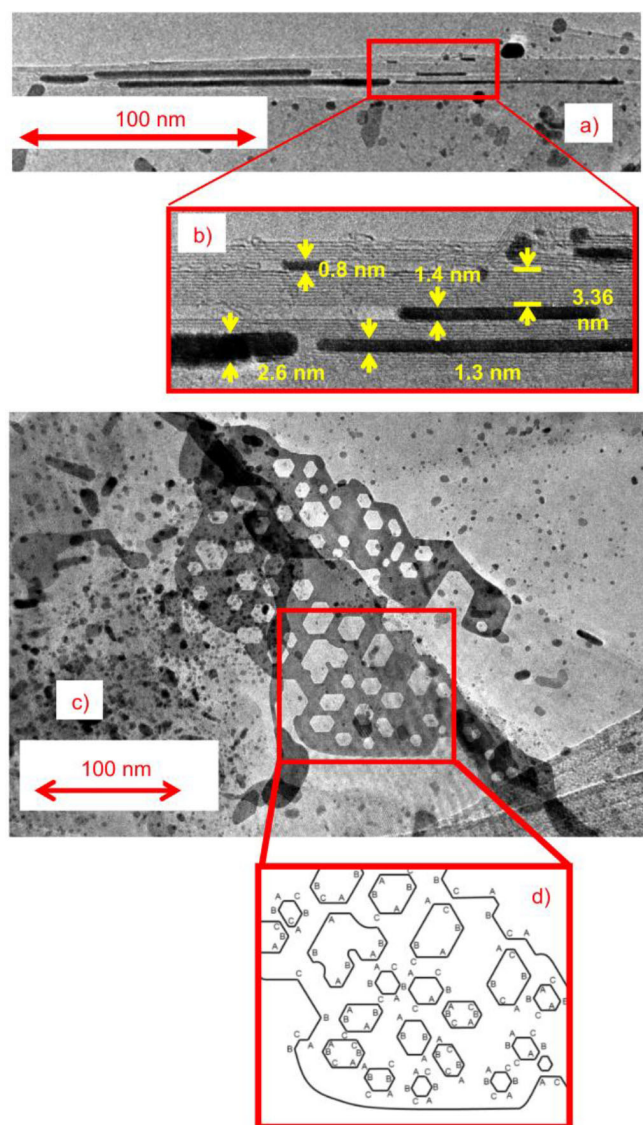


Figure 6. TEM images of 5Pt-GIC.

each other and the angles between two straight sides from three AB, BC, and AC directions are at 120° .

TEM images of 10Pt-GIC samples also showed the presence of platinum nanosheets which have a number of hexagonal holes and edges at angles of 120° (Figure 7). The size and thickness of the platinum nanosheets did not depend on the amount of platinum intercalated in the Pt-GIC samples.

When platinum particles are formed in the pores of supports, the morphology of the metal particles becomes the same as that of pores (a template method). For example, platinum nanowires are formed in the uniform mesotubes of folded-sheet mesoporous material FSM-16.^[19] One-dimen-

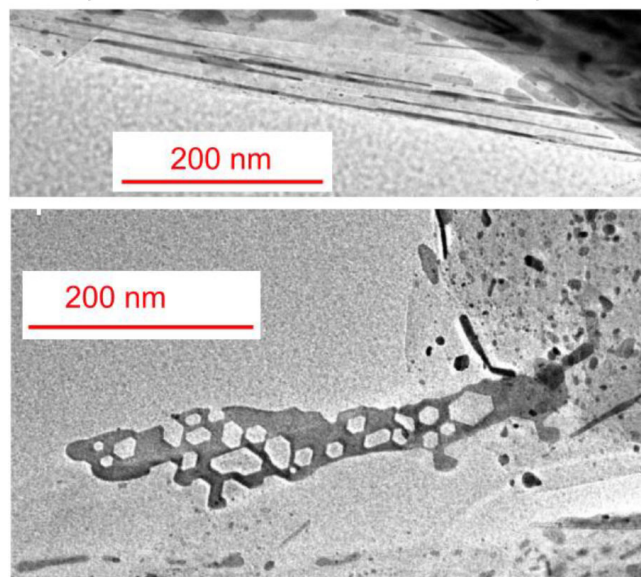


Figure 7. TEM image of 10Pt-GIC.

sional platinum clusters (platinum nanorods) are formed in the channels of carbon atoms.^[20] For the aggregation of platinum metal species between two-dimensional graphite layers, the interaction of graphite layer is not so high, hence the platinum nanosheets could enlarge the space between graphite layers.

The structure of the graphite layers would reflect on the peculiar structure (holes and edges) of the platinum nanosheets. Platinum atoms or platinum chloride molecules or both would migrate along with a regular hexagonal net of carbon atoms during hydrogen reduction at 573 K. Movement during the reduction would determine the morphology of the resulting platinum nanosheets, which have hexagonal holes.

The chlorine oxidation and hydrogen reduction behaviors were studied by the treatment of Pt-GIC with chlorine.^[21] 5Pt-GIC was treated with 0.3 MPa of chlorine at 723 K for 1 day to obtain an oxidized sample (5PtClx-GIC2) and 5PtClx-GIC2 was reduced at 40 KPa of hydrogen at 573 K to produce a reduced sample (5Pt-GIC2). The three peaks at $2\theta = 10.0^\circ$, 14.6° , and 20.3° were also observed in the X-ray diffraction patterns of 5PtClx-GIC2 and their intensities were almost the same as that of 5PtClx-GIC, indicating that platinum metal nanosheets were oxidized and platinum chloride species were formed between graphite layers with third stage structure. TEM images for 5Pt-GIC2 showed that platinum nanosheets with hexagonal holes were also formed. These results show that hydrogen reduction of platinum chloride to platinum nanosheets and chloride oxidation of

platinum nanosheets to platinum chloride were reversible between PtCl_x-GIC and Pt-GIC samples.

To study the chlorine oxidation process of platinum nanosheets, 5Pt-GIC was treated under 0.3 MPa of chlorine from room temperature to 473 K at the rate of 10 K/min. TEM image of the sample is shown in Figure 8. In addition to platinum metal sheets, small platinum particles, which are similar to those observed in the 5PtCl_x-GIC sample (Figure 4), are also observed. A part of platinum nanosheets would be oxidized to platinum chloride species, which were reduced to metal by the irradiation of electron beam during TEM observation. Besides the nanosheets, small platinum metal particles are also formed (Figure 8), which indicates that chlorine would intercalate between graphite layers and oxidize the nanosheets from the edge side. On the other hand, small platinum metal particles are also observed in the hexagonal holes and above (or below) of the nanosheets. One probable explanation for the oxidation of nanosheets from the inner side by chlorine is that voids would exist in a graphite layer (graphene) and chlorine molecules would pass through the voids and oxidize from the inner side of platinum sheets. The existence of the voids would be predicted by the reversibility of PtCl_x-GIC and Pt-GIC. Platinum nanosheets with 1–3 nm thickness could not be produced by the agglomeration of platinum atoms from one intercalant platinum chloride layer with third stage structure during reduction. Many platinum atoms would pass through the voids and aggregate to form platinum nanosheets with 1–3 nm thickness during the hydrogen reduction process. In the chlorine oxidation process, platinum chloride species derived from the nanosheets would pass through the voids to produce third stage structure.

3. Hydrogenation Catalysis of Pt-GIC

Platinum nanosheets, which have 1–3 nm thickness and 5–300 nm width, are located between expanded graphite layers

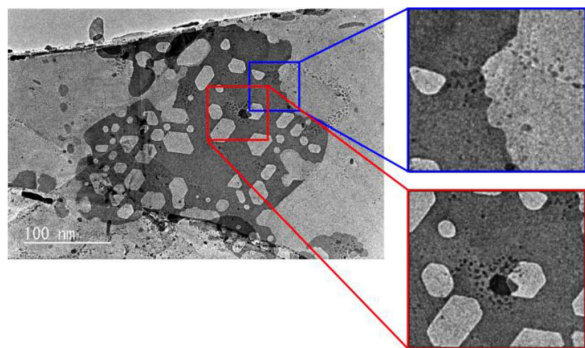


Figure 8. TEM image of 5Pt-GIC treated under 0.3 MPa of chlorine at from room temperature to 473 K at the rate of 10 K/min.

for Pt-GIC. For the application of Pt-GIC as solid catalysts, the active sites would be edges of the platinum sheets sandwiched between graphite layers. Compared with graphite-supported platinum catalysts (Pt/G), in which small platinum metal particles are located on graphite surface, the number of active sites of platinum nanosheets would be much smaller than that of small platinum metal particles on surface, then higher activities of Pt-GIC would not be expected.

On the other hand, it is expected that Pt-GIC would show differential selectivities compared with Pt/G. For the hydrogenation of planer unsaturated compounds over Pt-GIC, the planer molecules would enter into the two-dimensional expanded graphite layers and adsorb on the edge of the platinum nanosheets and be hydrogenated. The adsorption structure of the planer molecules to nanosheets in the two-dimensional space would be different from that to platinum particles on graphite surface, indicating that Pt-GIC would show different selectivities from Pt/G.

3.1. Phenylbenzene Hydrogenation

Benzene hydrogenation activities over 6.3Pt-GIC were compared with those over a commercially available charcoal supported platinum catalyst (5Pt/C) in ethanol solvent at 313 K under 4.0 MPa of hydrogen.^[22] Cyclohexane was the main product under the reaction conditions; however, the activities were different for 6.3Pt-GIC and 5Pt/C catalysts. 5Pt/C showed 33 and 42% conversion after 3 and 15 hours, respectively. On the other hand, the activity of 6.3Pt-GIC was very low at 0.4% for 3 hours. The conversion did not show any appreciable increase with an increase in reaction time and only 2.4% conversion was obtained over 6.3Pt-GIC after 15 hours. This result indicates that Pt-GIC is not active for the aromatic ring hydrogenation in ethanol.

The hydrogenation of phenylacetylene (PA), which has two kinds of unsaturated bonds (aromatic ring and carbon-carbon triple bond), was studied over 6.3Pt-GIC and commercially available supported platinum catalysts (5Pt/C and 5 wt% alumina-supported platinum (5Pt/Al₂O₃, WAKO Chemicals)) in ethanol solvent at 313 K (Table 1).^[22]

Three catalysts showed 100% conversion and the main product was ethylbenzene (EB) and minor ethylcyclohexane (EC), indicating that the hydrogenation rate of ethynyl group was faster than that of the aromatic ring under the present reaction conditions. Especially, the EC selectivity over 6.3Pt-GIC was much lower by more than one order of magnitude compared with the other two supported Pt catalysts for 3 h. After 15 h, the amounts of EC increased while, that of EB slightly decreased, indicating that only a small fraction of EB formed was further hydrogenated to EC. The results of phenylacetylene and benzene hydrogenation showed that the

Table 1. Hydrogenation of phenylacetylene for Pt-GIC and conventional supported Pt catalysts [a].

catalyst	time/ h	conversion/ %	product/mmol	
			ethylbenzene	ethyl- cyclohexane
6.3Pt-GIC	3	100	8.97	0.027
5Pt/ Al ₂ O ₃	15	100	8.90	0.10
5Pt/C	3	100	8.74	0.26
5Pt/C	15	100	8.62	0.38
5Pt/C	3	100	8.55	0.45
5Pt/C	15	100	8.36	0.64

[a] phenylacetylene 9.0 mmol, 6.3Pt-GIC 38 mg, 5Pt/Al₂O₃ 50 mg, 5Pt/C 50 mg, Reaction temperature 313 K, H₂ 4.0 MPa, ethanol solvent 4 cm³.

aromatic rings are difficult to be hydrogenated over Pt-GIC compared with the conventional supported Pt particles on the surface. The ethynyl group of phenylacetylene was hydrogenated with Pt-GIC, and so the two substrates, phenylacetylene and benzene can get an access to active sites of platinum nanosheets between graphite layers. However, the space between the graphite layers is limited and the periphery of the Pt nanosheets should be active sites; hence aromatic ring would be adsorbed in a mode of mono- or di- σ -adsorption while, the adsorption with the π -ring parallel to the Pt surface is unlikely to occur. The attack of hydrogen atoms to the aromatic rings is restricted from the side of π -ring because of the characteristic structure of Pt-GIC and they are difficult to be hydrogenated through such a side attack of hydrogen. In contrast, such effects are unlikely with the carbon-carbon triple bonds.

3.2. Cinnamaldehyde Hydrogenation

Commercially important selective hydrogenation of cinnamaldehyde (CAL) was studied over Pt-GIC in *n*-heptane and supercritical carbon dioxide (scCO₂) solvents. For comparison, spherical platinum metal particles on graphite surface were prepared by hydrogen treatment of the mixture of solid chloroplatinic acid hexahydrate and graphite powder (Pt/Gmix) and its activities were studied.

Figure 9 shows the conversion and the amounts of products for the CAL hydrogenation over 5Pt-GIC and 5Pt/Gmix in *n*-heptane solvent.^[23] Both the catalysts showed hydrogenation activities; however, the hydrogenation rate is not so high over 5Pt-GIC. Hydrocinnamaldehyde (SAL), cinnamyl alcohol (UOL) and hydrocinnamyl alcohol (SOL) were formed after 30 minutes and dehydroxylation products of β -methyl styrene (MS) and small amount of propylbenzene (PB) were formed after 45 min.

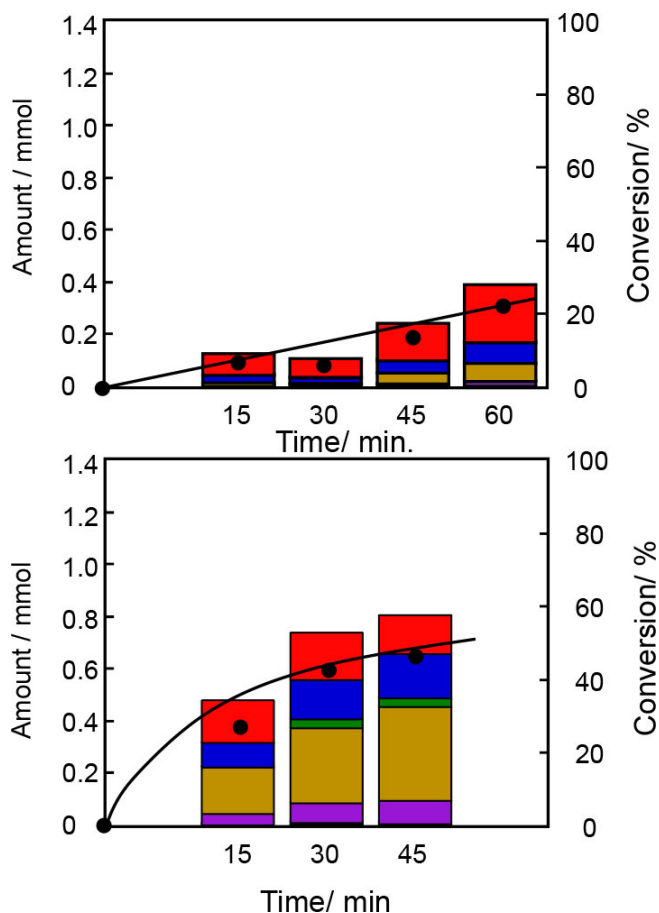


Figure 9. Cinnamaldehyde hydrogenation over 5Pt-GIC (a) and 5Pt/Gmix (b) under 5 MPa of hydrogen in *n*-heptane at 373 K (red: cinnamyl alcohol (UOL), blue: hydrocinnamaldehyde (SAL), and green: hydrocinnamyl alcohol (SOL), brown: β -methyl styrene (MS), purple: propylbenzene (PB), and black: cinnamic acid (CA)).

UOL was the main product and the UOL selectivity was almost constant at around 60% and independent of reaction rate up to 60 min. The selectivity to dehydroxylated product of MS and PB was 24% in 60 min. Figure 9(b) shows the hydrogenation activity over 5Pt/Gmix, which showed high CAL activity; however, lower UOL selectivity (33%) was observed over 5Pt/Gmix. The selectivity to dehydrogenated by-products (MS and PB) over 5Pt/Gmix was higher (50%) as compared with that over the Pt-GIC sample. The lower CAL conversion over 5Pt-GIC shows that the lower number of exposed platinum metal sites of platinum nanosheets existed between graphite layers. Spherical platinum metal particles are exposed on graphite surface and CAL molecules easily accessed the active sites over 5Pt/Gmix. It was hardly possible to determine the number of Pt atoms located at the edge of Pt nanosheets; however, it is not difficult to project that the number of edge sites in Pt nanosheets between

graphite layers (Pt-GIC) would be much smaller than that of surface atoms of platinum particles on graphite (Pt-Gmix). The turn number of nanosheets in Pt-GIC may be larger than that of small particles on graphite in Pt-Gmix.

5Pt-GIC showed higher UOL selectivity compared with that shown by 5Pt/Gmix. For similar conversion of around 25% (in 60 min over Pt-GIC and 15 min over Pt/Gmix), the UOL selectivity over Pt-GIC (56%) were also higher than that over Pt/Gmix (33%). The higher COL selectivity over 5Pt-GIC shows that the preferential adsorption of carbonyl group of CAL molecule takes place on the exposed Pt metal sites on nanosheets intercalated graphite layers because the adsorption of C=C group of CAL molecule was hindered by the steric factors between phenyl group and graphite layers in the 5Pt-GIC samples. Such hindrance was not possible in the hydrogenation over 5Pt/Gmix because Pt metal particles are arranged on the graphite layers and selectivity to SAL became high and SOL was also formed over 5Pt/Gmix samples. Also, the amounts of dehydroxylated by-product of MS and PB were formed to the larger extent over Pt/Gmix.

Figure 10 shows the hydrogenation profile over 5Pt-GIC and 5Pt/Gmix under 5 MPa of hydrogen and 10 MPa of scCO₂ at 323 K.^[18] Both 5Pt-GIC and 5Pt/Gmix catalysts showed higher hydrogenation activities in scCO₂ than in *n*-heptane at 373 K, especially the activity in scCO₂ was much higher than in *n*-heptane over 5Pt-GIC. The higher activities in scCO₂ could be explained by the higher hydrogen concentration on platinum sites than in *n*-heptane under the same hydrogen pressure at 323 K. Hydrogen is completely miscible with scCO₂, hence, higher amount of hydrogen atoms would be available on the platinum metal surface in scCO₂ and hydrogenation would proceed on both over Pt-GIC and Pt/Gmix catalysts. It is reported that graphite layers could be exfoliated by scCO₂ treatment,^[24] indicating that carbon dioxide molecules enter into graphite layers. Carbon dioxide molecules under supercritical conditions may enter into graphite layers and also carry CAL molecules to platinum nanosheets between the layers, resulting in higher hydrogenation activities over 5Pt-GIC in scCO₂ than in *n*-heptane. The high UOL selectivity was also obtained over 5Pt-GIC in scCO₂. The UOL selectivity was almost constant at 77% and independent of reaction rate up to 240 min over 5Pt-GIC. Dehydroxylation products (MS and PB) were not formed at the beginning of the reaction. Total selectivity for hydrogenated compounds (UOL + SAL + SOL) were more than 98% at 360 min. Over Pt/Gmix, the UOL selectivity values were lower than 50% and large amount of the dehydroxylation byproducts (MS and PB) was formed.

4. Summary and Outlook

Platinum nanosheets were synthesized by the hydrogen reduction of platinum tetrachloride intercalated between graphite layers. The dimensions of platinum nanosheets were 1–3 nm in thickness with 5–300 nm width. There are a number of hexagonal holes and edges with 120° angle in the platinum nanosheets. The hydrogenation performance (activity and selectivity) of platinum nanosheets between graphite layers were different from those of spherical platinum metal particles supported on graphite layers.

Several noble metal sheets with nanosize thickness could be synthesized by the reduction of the corresponding noble metal chloride intercalated between graphite layers. Also, bimetallic nanosheets could be prepared by the reduction of binary metal chlorides intercalated between graphite layers. The noble metal nanosheets and bimetallic nanosheets would show the different catalysis from those of supported mono-metal and bimetallic particles.

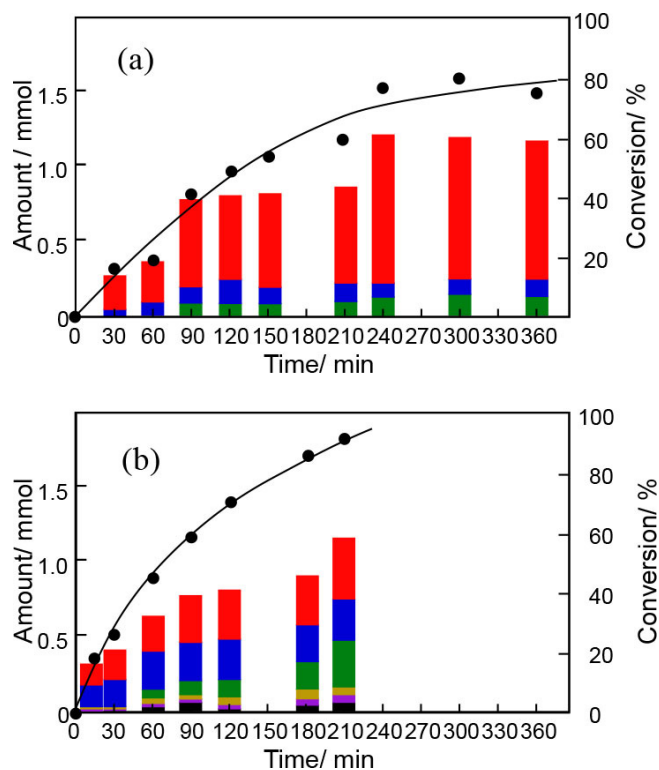


Figure 10. Cinnamaldehyde hydrogenation over 5Pt-GIC (a) and 5Pt/Gmix (b) under 5 MPa of hydrogen in 10 MPa of supercritical carbon dioxide solvent at 323 K (red: cinnamyl alcohol (UOL), blue: hydrocinnamaldehyde (SAL), and green: hydrocinnamyl alcohol (SOL), brown: β-methyl styrene (MS), purple: propylbenzene (PB), and black: cinnamic acid (CA)).

Acknowledgements

This work was supported by Grand-in-Aid (18H01782) for Scientific Research B from Ministry of Education, Culture, Sports, Science and Technology of Japan.

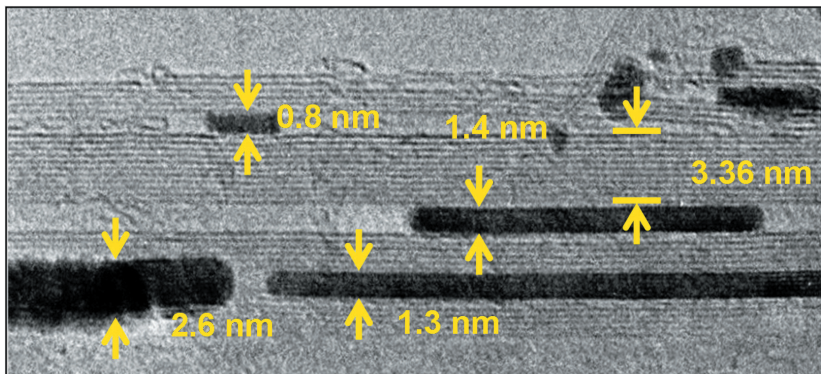
References

- [1] M. S. Dresselhaus, G. Dresselhouse, *Adv. Phys.* **2002**, *51*, 1–186
- [2] H. Klotz, A. Schneider, *Naturwissenschaften*, **1962**, *49*, 448
- [3] M. E. Vol'pin, Yu. N. Novikov, N. D. Lapkina, V. I. Kasatochkin, Yu. T. Struchkov, M. E. Kazakov, R. A. Stukan, V. A. Povitskij, Yu. S. Karimov, A. V. Zvarikina, *J. Am. Chem. Soc.* **1975**, *97*, 3366–3373
- [4] G. Sirokman, A. Mastalir, A. Molnar, M. Bartok, Z. Schay, L. Guzzi, *J. Catal.* **1989**, *117*, 558–560.
- [5] A. Furstner, F. Hofer, H. Weidmann, *J. Catal.* **1989**, *118*, 502–506.
- [6] G. Sirokman, A. Mastalir, A. Molnar, M. Bartok, Z. Schay, L. Guzzi, *Carbon* **1990**, *28*, 35–42.
- [7] F. Notheisz, A. Mastalir, M. Bartok, *J. Catal.* **1992**, *134*, 608–614.
- [8] A. Mastalir, F. Notheisz, M. Bartok, T. Haraszti, Z. Kiraly, I. Dekany, *Appl. Catal. A* **1996**, *144*, 237–248.
- [9] Z. Kiraly, A. Mastalir, F. Berger, I. Dekany, *Langmuir* **1997**, *13*, 465–468.
- [10] D. Mendoza, F. Morales, R. Escudero, J. Walter, *J. Phys. Cindens. Matter* **1999**, *11*, L317-L322.
- [11] J. Walter, H. Shioyama, *Phys. Lett. A* **1999**, *254*, 65–71.
- [12] M. Shirai, K. Igeta, M. Arai, *Chem. Commun.* **2000**, 623–624.
- [13] M. Shirai, K. Igeta, M. Arai, *J. Phys. Chem. B* **2001**, *105*, 7211–7215.
- [14] C. V. Rode, U. D. Joshi, O. Sato, M. Shirai, *Chem. Commun.* **2003**, 1960–1961.
- [15] M. Arai, S. Fujita, M. Shirai, *J. Supercrit. Fluids* **2009**, *47*, 351–356.
- [16] M. F. Pilbrow, *Chem. Commun.* **1973**, 270–271.
- [17] P. M. F. J. Costa, J. Sloan, T. Rutherford, M. L. H. Green, *Chem. Mater.* **2005**, *17*, 6579–6582.
- [18] H. Amanuma, H. Nanao, M. Shirai, *Chem. Lett.* **2018**, *47*, 475–478.
- [19] M. Sasaki, N. Higashino, A. Fukuoka, M. Ichikawa, *Micro. Meso. Mater.* **1998**, *21*, 597–606.
- [20] T. Kyotani, L. Tai, A. Tomita, *Chem. Commun.* **1997**, 701–702.
- [21] M. Shirai, Y. Yamazaki, K. Takahashi, H. Nanao, *Chem. Lett.* **2018**, *47*, 1094–1096.
- [22] M. Shirai, B. M. Bhanage, H. Senboku, S. Fujita, M. Arai, *J. Jpn. Pet. Inst.* **2002**, *45*, 420–421.
- [23] M. Horie, K. Takahashi, H. Nanao, N. Hiyoshi, M. Shirai, *J. Nanosci. Nanotechnol.* **2018**, *18*, 80–85.
- [24] H. S. Sim, T. A. Kim, K. H. Lee, M. Park, *Mater. Lett.* **2012**, *89*, 343–346.

Manuscript received: July 2, 2018

Version of record online: November 20, 2018

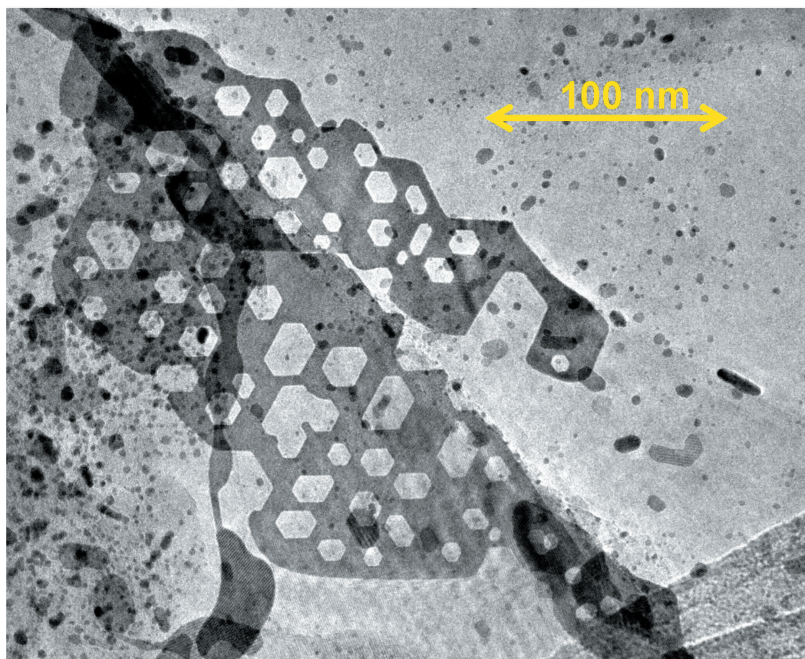
PERSONAL ACCOUNT



*Prof. M. Shirai**

1 – 10

**Platinum Nanosheets between
Graphite Layers**



In this account, we discuss the preparation and structure of two-dimensional platinum nanosheets intercalated between graphite layers. The size of platinum nanosheets was 1–3 nm in thickness with a width in the range of 5–300 nm. These

nanosheets contain a number of hexagonal holes and edges with an angle of 120° . The selective hydrogenation catalyzed by these platinum nanosheets entrapped between the graphite layers is also demonstrated.
